journal

J. Am. Ceram. Soc., **82** [11] 3139–44 (1999)

Mechanical Properties of Textured $Bi_2Sr_2CaCu_2O_{8+\delta}$ High-Temperature Superconductors

Jose Ygnacio Pastor, Pedro Poza, and Javier LLorca*

Department of Materials Science, Polytechnic University of Madrid, E.T.S. de Ingenieros de Caminos, 28040 Madrid, Spain

The mechanical properties of $Bi_2Sr_2CaCu_2O_{8+\delta}$ fibers produced via laser-induced directional solidification at different growth rates were determined through longitudinal and transverse tension tests, as well as flexure tests. In addition, polished sections of as-received fibers and the fracture surfaces of the broken samples were examined using scanning electron microscopy to elucidate the relationship between the microstructure and the mechanical properties. The fibers were anisotropic, and the transverse fiber strength was very low, because of early failure via cleavage of the grains perpendicular to the *c*-axis. The longitudinal strength and the degree of anisotropy increased as the fiber growth rate decreased, whereas the transverse strength followed the opposite trend. This behavior was due to changes in the porosity and the alignment of the crystals along the fiber axis.

I. Introduction

HIGH-TEMPERATURE ceramic superconductors (HTCSs) exhibit very poor mechanical properties, which may hinder their application in components that are subjected to significant thermal stresses, such as current leads, current limiters, and level sensors in cryogenic fluids. The flexure strength of pressureless-sintered $YBa_2Cu_3O_{7-\delta}$ (YBCO) bars is 20–90 MPa, whereas the fracture toughness is ~1.0–2.0 MPa·$m^{1/2}$.[1–3] The low strength and toughness, as well as the scatter in the properties, are attributed to the porosity and the development of microcracking upon cooling from the sintering temperature, because of the thermal stresses that are generated by the thermoelastic anisotropy of the crystal. The strength and toughness of pressureless-sintered $Bi_2Sr_2CaCu_2O_{8+\delta}$ (BSCCO 2212) superconductors are even lower than those measured on YBCO bars,[3,4] as densification is more difficult because the grains are in the form of thin plates. Marked improvements in the flexure strength of YBCO (up to 120–190 MPa) and BSCCO 2212 (~90 MPa) superconductors can be obtained using other processing techniques, such as extrusion,[5] hot isostatic pressing,[6] and sinter forging,[7] which significantly reduces the porosity. Similar results have been reported in $Bi(Pb)_2Sr_2Ca_2Cu_2O_{8+\delta}$ (BSCCO 2223) materials that were processed using hot pressing[8] and sinter forging,[4] whose respective flexure strengths reached 110 and 135 MPa.

BSCCO superconductors that have been manufactured by hot pressing and sinter forging exhibit a textured microstructure. The platelike orthorhombic grains grow mainly in the crystallographic *ab* planes, with the ***c***-axis [001] parallel to the pressing or forging direction.[7,8] This anisotropy influences the superconducting properties, because the critical current density (J_c) in the *ab* plane is much higher than that along the ***c***-axis. For instance, Goretta *et al.*[4] measured J_c values of 1 and 8 kA/cm^2 in pressureless-sintered and sinter-forged BSCCO 2223 bars, respectively, at 77 K and zero external field. These preliminary investigations also detected the anisotropy in the mechanical properties of BSCCO superconductors, which fail easily via cleavage in planes perpendicular to the ***c***-axis.[7,8] However, the above-mentioned strength data were obtained mainly through bending tests, and it was not possible to determine the degree of anisotropy from these results. The purpose of this investigation was to measure the actual tensile strength in the longitudinal and transverse directions in textured HTCSs and correlate the mechanical behavior with the microstructure. These properties are critical in the mechanical design, and it should be emphasized that the reduced transverse strength of HTCSs could compromise the reliability of BSCCO components, which may fracture by splitting under the action of the thermal stresses that are generated during operation.

The longitudinal and transverse strengths were measured on textured BSCCO 2212 fibers that were manufactured via laser-induced directional solidification.[9–11] The tightly focused coherent laser radiation induces extreme temperature gradients at the solidification interface, which leads to directional crystal growth in the fiber direction. This technique has demonstrated its capability to produce textured BSCCO 2212 fibers with J_c values of >5 kA/cm^2 at 80 K[10] and >60 kA/cm^2 at 68 K and zero external field.[11] The mechanical characterization was completed with the determination of the elastic modulus and the flexure strength. In addition, polished sections of as-received fiber and the fracture surfaces of the broken samples were examined via scanning electron microscopy (SEM), to elucidate the relationship between the microstructure and the mechanical properties.

II. Materials

Textured BSCCO 2212 fibers ~2 mm in diameter and >10 cm in length were manufactured using laser-induced directional solidification.[9–11] Powders of Bi_2O_3, $SrCO_3$, $CaCO_3$, and CuO were mixed in the appropriate amounts to obtain an ideal stoichiometry. The resulting mixture was calcined at 1073 K for 1 h, ground, and then cold isostatically pressed inside latex tubes to form circular bars. The bars were fed at constant speed into a growth chamber, where they were transformed to textured fibers using a neodymium–yttrium aluminum garnet (Nd:YAG) laser that was focused symmetrically around the bars in a dry-air atmosphere. The localized laser radiation produces a short molten zone, where the temperature gradients at the solidification interface are very high (10^5–10^6 K/m). The molten region is maintained in an equilibrium state by the surface tension between the feed bar and the textured fiber, and it is displaced at the feeding rate along the fiber, which leads to directional crystal growth. The textured fibers finally were an-

R. K. Bordia—contributing editor

Manuscript No. 190172. Received May 22, 1998; approved May 17, 1999.

Supported by CICYT, Madrid, Spain (through Grant No. MAT97-673-C02) and CICYT and the European Union (through Grant No. 2FD97-546). Processing of the materials used in this study was conducted at Ciencia de Materiales de Aragón, which was supported by CICYT (through Grant No. MAT95-921) and Red Eléctrica de España (through Project No. REE-ID-97017).

*Member, American Ceramic Society.

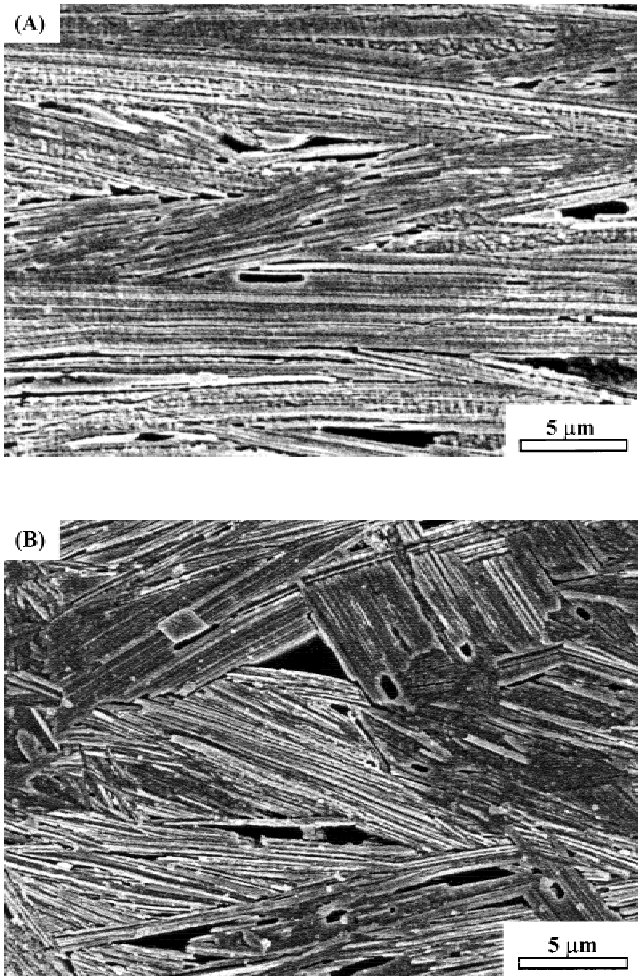

Fig. 1. SEM micrographs of the microstructure of material A fiber, grown at a rate of 10 mm/h ((A) longitudinal and (B) transverse section).

nealed in air at 1118 K for 96 h. The superconducting critical temperature for the textured fibers, which was defined by the onset of diamagnetism, was ~90 K, whereas the J_c values in the longitudinal direction at 77 K and zero applied field were 2–3.5 kA/cm^2. More details about the processing techniques and transport properties can be found elsewhere.[9,12]

Three BSCCO 2212 fibers were processed for this investigation, using different feeding rates: 10 mm/h (material A), 30 mm/h (material B), and 70 mm/h (material C). The feed bar and the textured fiber rotated in opposite directions at a speed of 15 rpm during the process. The microstructure of the material A fiber in the longitudinal and transverse directions is shown in Figs. 1(A) and (B). The orthorhombic superconductor grains grew with the crystallographic *ab* planes oriented approximately in the fiber direction.[11] They were arranged in domains of aligned grains, which resulted from the piling of flat grains whose thickness in the ***c***-axis was ~0.2 μm. The total domain thickness was 2–10 μm (Fig. 1(A)). Pores were observed at the intersections between misaligned domains. Micrographs of the transverse section showed that the domains were randomly oriented in the radial direction and that porosity also was concentrated at the intersections between domains (Fig. 1(B)).

Three fibers, each ~15 mm in length, were used to measure the density of each material; the Archimedes method was used, with ethanol as the medium. The results, together with the corresponding standard errors, are shown in Table I. The density increased as the feeding rate decreased, reaching a density of 95% of the BSCCO 2212 theoretical density (6.6 g/cm^3) for the fibers grown at 10 mm/h (material A). This effect is partially due to the improvement in grain alignment in the longitudinal direction at slower growth rates, which reduces the volume fraction of pores at the intersection between misaligned domains.[13] In addition, the air bubbles that are trapped in the molten solid may escape more easily when the speed at the solidification interface decreases. Spherical pores induced by these bubbles were observed in the fracture surfaces of the specimens that were tested in tension, and their influence on the mechanical properties is discussed in the Results section.

III. Experimental Techniques

The tensile strengths of the superconductor fibers in the longitudinal and transverse directions were measured in a servomechanical testing machine (Model 4505, Instron, Ltd., High Wycombe, U.K.). Duplicate tests for each material were performed to determine the tensile strength in the longitudinal direction, using fibers of 30 mm in length. The experimental setup is shown in Fig. 2(A). The fiber ends were introduced into cylindrical cavities that were machined in aluminum heads. The cavity diameter was 0.1 mm greater than that of the fibers, and the superconductors were glued to the aluminum using cyanoacrylate. The free length of the fibers between the aluminum heads was ~10 mm. The aluminum heads were connected to the actuator and the load cell of the testing machine using nylon cords, which provided a very flexible loading system that ensured that the bending and torsional stresses on the superconducting fibers were negligible. The tests were performed under stroke control at a crosshead speed of 2 mm/min. The dynamic elastic modulus of the rods in the longitudinal direction was determined using the flexural-vibration resonance method on fibers of 30 mm in length (Model Grindosonic MK4i, J. W. Lemmens, Belgium). The frequency of resonance in these tests was ~8500 Hz.

The transverse strength of the superconductor fibers was obtained using the diametral compression test (also known as the Brazilian test), which is a standard procedure to measure the tensile strength of concrete.[14] Circular disks 1.2 mm thick were cut from the rods and subjected to diametral compression between two rigid ceramic plates (Fig. 2(B)). The tests were performed under stroke control at a crosshead speed of 12 μm/min. Assuming that the material is linear elastic and that the contact area between the disk and the plates is very small (in comparison to the disk diameter, D), the stress perpendicular to the compressed diameter is tensile and constant along the diameter. The stress (σ) is given by

$$\sigma = \frac{2P}{\pi DB} \tag{1}$$

where P is the compressive load and B the disk thickness. Although the compressive stresses in the load direction are much higher than the transverse tensile stresses, the disk fails

Table I. Growth Rates, Densities, and Mechanical Properties of the Fibers

Material	Growth rate (mm/h)	Density, ρ (g/cm^3)	Longitudinal elastic modulus, E_l (GPa)	Longitudinal strength, σ_l (MPa)	Transverse strength, σ_t (MPa)	Flexure strength, σ_f (MPa)
A	10	6.26 ± 0.01	101 ± 6	43 ± 3	7.5 ± 0.6	139 ± 14
B	30	6.12 ± 0.02	101 ± 3	34 ± 2	6.4 ± 0.3	120 ± 7
C	70	5.97 ± 0.04	93 ± 4	26 ± 1	10.9 ± 0.4	117 ± 3

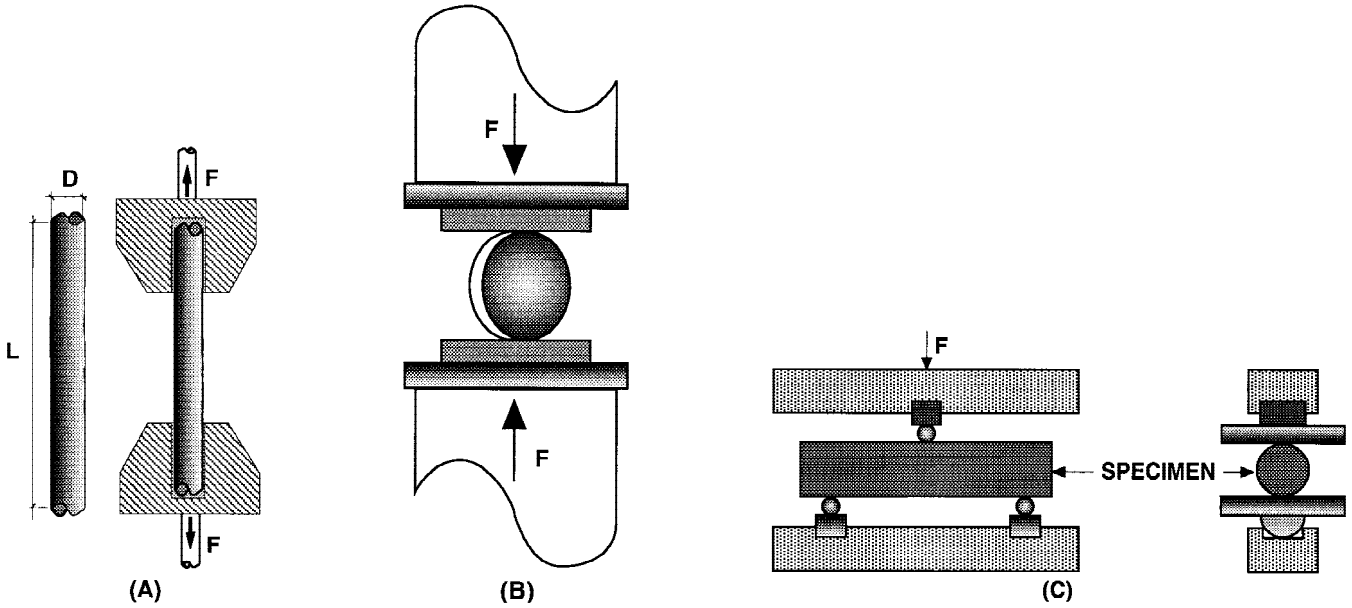

Fig. 2. Scheme of the experimental setup ((A) longitudinal tension tests, (B) diametral compression tests, and (C) flexure tests).

by splitting along the compressed diameter in ceramic materials and concrete, where the compressive strength is significantly higher than the tensile strength. At least nine disks of each material were tested.

Triplicate three-point-bend flexure tests on each material also were performed on the superconductor rods, for comparison with the literature data, because all the strength measurements in high-temperature superconductors that have been reported to date were obtained in bending.[1–8] The span of the loading fixture was 5 mm, and the experimental setup for this procedure is shown in Fig. 2(C). The tests were performed under load control at a loading rate of 10 N/min. The flexure strength was computed from the maximum load in the test, according to the strength of materials theory for an elastic beam of circular cross section.

The fracture surfaces of the samples broken in direct and transverse tension, as well as in flexure, were examined via SEM (Model JSM 6300, JEOL, Tokyo, Japan) to ascertain the dominant failure mechanisms. In addition, longitudinal and transverse sections of the as-received fiber were polished and chemically etched at 300 K for 60 s with a mixture of 99% 2-butoxyethanol and 1% perchloric acid (60% concentration) to reveal the microstructure. Then, they were examined via SEM (see Fig. 1).

IV. Results and Discussion

The flexure strength (σ_f) of the fibers is shown in Fig. 3(A), whereas the tensile strengths in the longitudinal (σ_l) and transverse (σ_t) directions are plotted in Fig. 3(B). The average values of these magnitudes, and the corresponding standard errors, are shown in Table I. The dynamic elastic modulus in the longitudinal direction (E_l), measured via the flexural vibration resonance technique, also is included in Table I. Three main conclusions can be drawn from these results. Firstly, the flexure strength of BSCCO fibers processed using laser-induced directional solidification was as good as or even better than that reported for other textured BSCCO materials.[7,8] Secondly, the longitudinal strength of the bars was significantly lower than the flexure strength for the three materials that were tested. Thirdly, the diametral compression tests revealed the anisotropy in the mechanical properties, and the transverse strengths were markedly lower than the longitudinal values. The extremely low transverse strength of these textured HTCSs is worth noting.

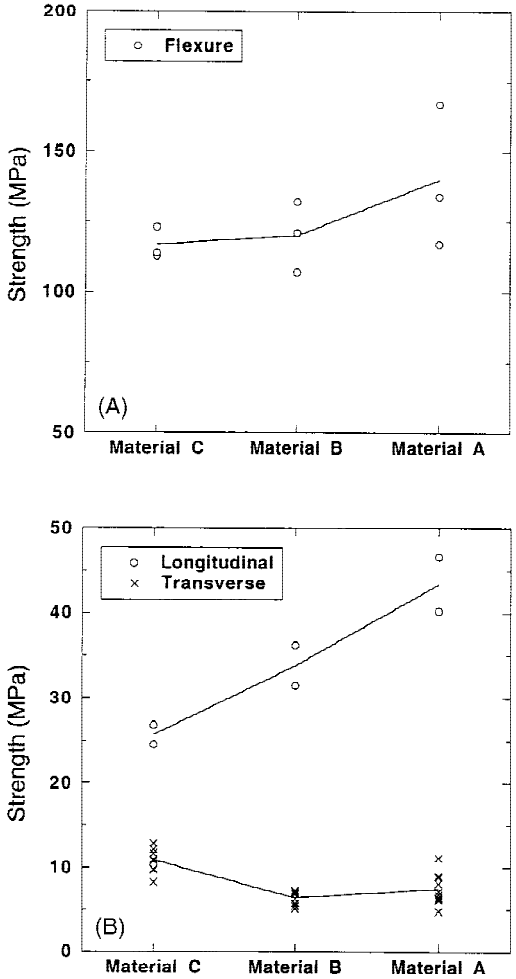

Fig. 3. (A) Flexural strength and (B) longitudinal and transverse tensile strengths of the fibers.

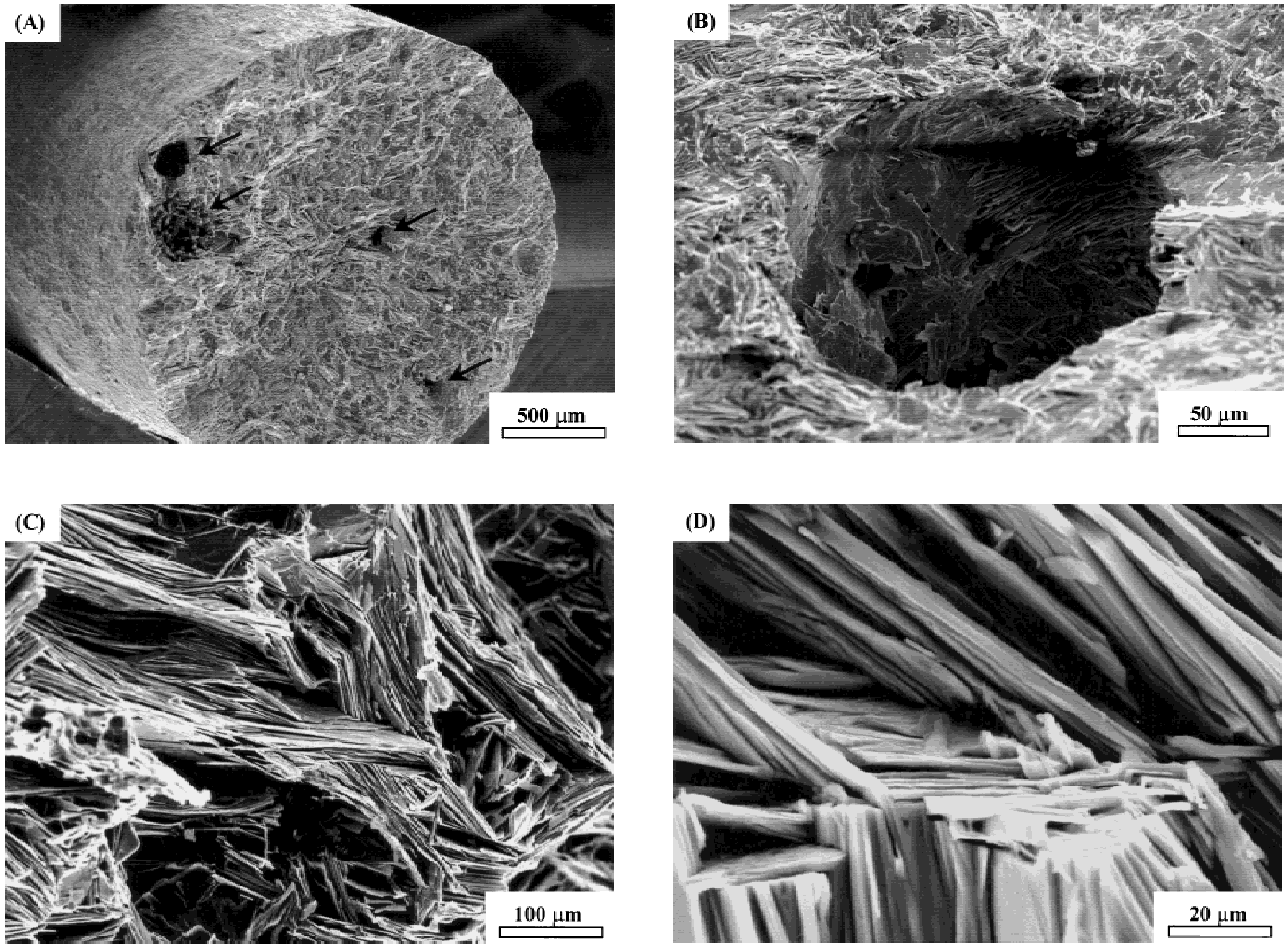

Fig. 4. Fracture surfaces of material A fibers broken in longitudinal tension ((A) low-magnification micrograph (pores are marked with arrows); (B) detail of an almost-spherical pore; (C) domains broken in tension; and (D) detail of a broken domain, showing delamination between the grains in each domain).

The failure strength of brittle ceramics is dictated by the size of the critical defect at which fracture is initiated. They usually exhibit lower strength in tension than in flexure, because the volume of material that is subjected to the maximum stress is larger in tension than in bending, and, thus, so is the probability of finding a critical defect. However, the differences for the BSCCO fibers are larger than expected, and this result may be induced by a wide distribution of defects in the fibers, with small and large defects dispersed throughout the material. This phenomenon should lead to significant scatter in the experimental data and very low values of the Weibull modulus (m). The number of tensile and flexure tests was not enough to compute the value of m; however, the scatter in the strength values and the defect population in the fibers (which is shown below) are consistent with this hypothesis and seem to indicate that the Weibull modulus for the fiber strength was very low.

The rate at which the fibers were grown had little influence on the flexure strength, although both the average strength and the scatter seemed to increase as the growth rate decreased. However, the longitudinal and transverse tensile strengths did change with the fiber growth rate, and their variations were opposed. The longitudinal strength increased ~65% whereas the transverse strength was reduced by >30% when the growth rate decreased from 70 mm/h to 10 mm/h. As a result, the degree of anisotropy in the fibers, which is defined as σ_l/σ_t, increased from 2.4 to 5.7.

The fracture surfaces of the fibers tested in longitudinal tension were macroscopically flat, and their analysis at low magnification showed the presence of large pores, such as those marked with arrows in Fig. 4(A). The pores were almost spherical (Fig. 4(B)), and they probably originated from bubbles that were trapped within the fiber during solidification. Specimen failure occurred as the domains of aligned grains were fractured perpendicular to the loading axis. The broken domains, which were randomly oriented in the radial direction, were clearly visible at the microscopic level on the fracture surfaces (Fig. 4(C)). Analysis of these domains at higher magnification showed that decohesion between the individual grains of each domain occurred during deformation (Fig. 4(D)), which revealed their layered structure.

This latter observation reveals the weak bonding between the grains along the ***c***-axis, which was responsible for the poor transverse strength of the BSCCO fibers. The fracture surfaces of the specimens that were tested under diametral compression also were macroscopically flat. However, analysis of these fracture surfaces at higher magnification showed the presence of smooth and rugged regions of an average size that was analogous to the domain size (Fig. 5(A)). They were dispersed throughout the fracture surface. The smooth regions were produced via cleavage of the grains between Bi_2O_2 layers that consisted of two parallel, planar BiO sheets (Fig. 5(B)). The Bi–O bonds between adjacent layers are strongly distorted, which leads to a large (~0.31 nm) interlayer spacing, which considerably reduces the binding forces and facilitates interlayer decohesion.[15,16] The rugged regions were formed by broken domains that protruded from the fracture surface (Fig. 5(C)), and their morphology was similar to that shown in Fig. 4(C) for the fractured domains in the specimens that were

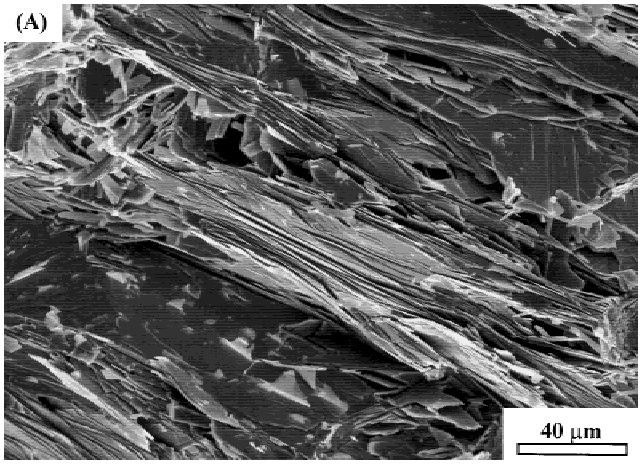

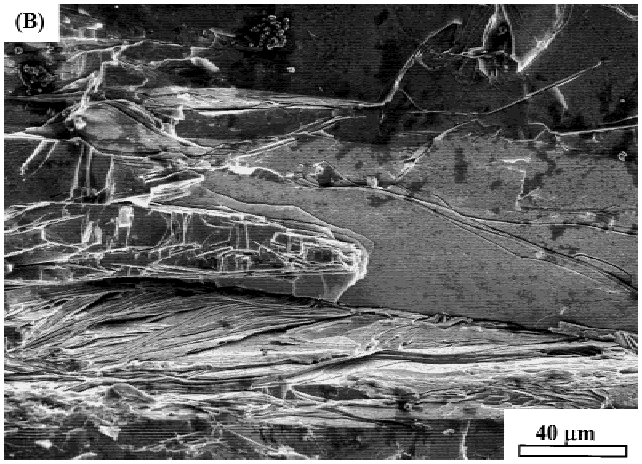

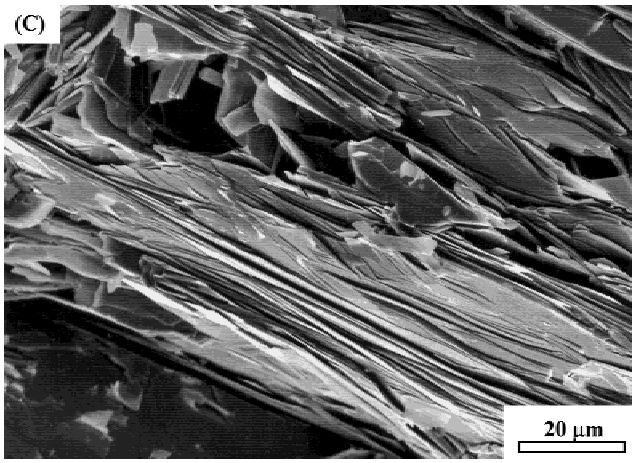

Fig. 5. Fracture surfaces of material A fibers broken in transverse tension, showing (A) the presence of smooth and rugged regions on the fracture surface, (B) the detail of a smooth region produced by cleavage of the grains between Bi_2O_2 layers that consisted of two parallel planar BiO sheets, and (C) the detail of a rugged region (delamination between the grains in the domain can be observed).

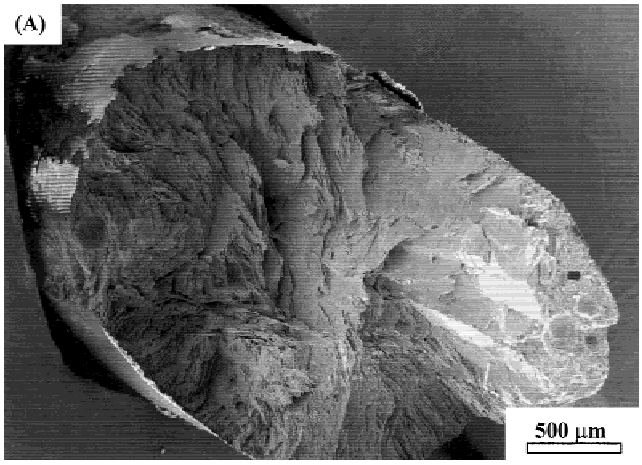

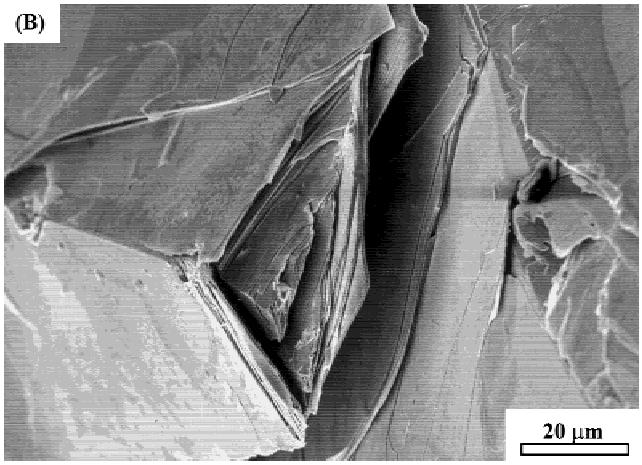

Fig. 6. Fracture surfaces of a material A fiber broken in bending ((A) macroscopic appearance, showing the coexistence of grains broken in the longitudinal direction with failure by delamination along the fiber axis, and (B) detail of a smooth fracture surface produced by delamination).

tested in longitudinal tension. Thus, the failure process in diametral compression was initiated at very low stresses via the nucleation of cracks by cleavage between Bi_2O_2 layers in domains whose ***c***-axis was approximately oriented in the direction of the transverse tensile stress. The final fracture occurred via the propagation of these cracks through the domains with the ***c***-axis aligned approximately perpendicular to the tensile stresses.

The mechanical tests indicate that the longitudinal strength increased as the fiber growth rate decreased; this observation may be explained by two factors. Firstly, the volume fraction of spherical pores within the fiber increases with the fiber growth rate. These pores, which are clearly visible on the fracture surface of material C (Figs. 4(A) and (B)), act as stress concentrators that help to initiate the fracture process at lower stress levels. Secondly, the alignment of the domains in the fiber direction improves as the growth rate is decreased;[13] thus, the fraction of domains with the *ab* planes parallel to the fiber axis is a maximum value for material A. The SEM analysis of the polished longitudinal sections of the fibers was qualitatively consistent with this result, but quantitative measurements of the degree of misalignment were not, possibly because of the low contrast among the domains. Indirect evidence of the better alignment of the *ab* planes along the fiber axes was provided by the longitudinal elastic moduli E_l (Table I). The elastic moduli of BSCCO 2212 single crystals along the *ab* plane and the ***c***-axis were 101 and 44 GPa,[17] respectively, because the large interlayer spacing between the BiO sheets along the ***c***-axis considerably reduced the crystal stiffness in this direction. The E_l values of materials A and B were similar to the single crystal value for the *ab* planes, whereas E_l for material C was ~10% lower.

These explanations also are consistent with the results for the

transverse tensile strength, which increased as the fiber growth rate increased. The lowest σ_t was obtained for materials A and B, where the *ab* planes were better aligned in the fiber direction; thus, the weak ***c***-axis of the crystal were oriented in the transverse directions. According to E_l, the alignment was similar in both fibers and they exhibited the same transverse strength (within the experimental scatter). In contrast, the degree of alignment was lower for the material C fiber, and this material presented the best transverse strength.

Thus, the fiber anisotropy increased as the growth rate decreased; this result was manifest on the fracture surfaces of material A tested in bending (Fig. 6(A)). They exhibited a very irregular morphology where grains that were broken in the longitudinal direction coexisted with failure by delamination along the fiber axis. The smooth fracture surface that is produced via cleavage of the grains between Bi_2O_2 layers during delamination is interesting to observe (Fig. 6(B)). The simultaneous presence of both fracture mechanisms could be partially responsible for the large scatter in the bending strength that is observed in material A.

V. Conclusions

The longitudinal and transverse strengths, as well as the bending strength, were measured on textured $Bi_2Sr_2CaCu_2O_{8+\delta}$ (BSCCO) high-temperature superconductor fiber produced via laser-induced directional solidification, using different growth rates. The bending strength of the fibers was as good as or even better than that reported for BSCCO superconductors that had been processed via hot pressing or sinter forging. The fibers were anisotropic: the longitudinal strength was 26–43 MPa, whereas the transverse strength was 6–11 MPa, and the degree of anisotropy increased as the fiber growth rate decreased. The reduced fiber strength in the transverse direction was due to the early failure via cleavage of the grains between Bi_2O_2 layers that consisted of two parallel, planar BiO sheets that were oriented perpendicular to the ***c***-axis of the crystal.

The improved longitudinal strength of the fiber growth at slower rates was mainly due to the reduction in the number and size of spherical pores that originated from bubbles that were trapped within the fiber during solidification. In addition, the alignment of the strong *ab* planes of the orthorhombic crystals in the fiber direction improved as the growth rate decreased, and this alignment also helped to increase the longitudinal strength. In contrast, as the strong *ab* planes were better aligned in the fiber direction, the weak ***c***-axis of the crystal were oriented in the transverse directions and the transverse strength decreased.

Acknowledgments: The authors thank J. C. Diez and L. A. Angurel (Instituto de Ciencia de Materiales de Aragón) for processing the materials that were used in this study.

References

[1]J. P. Singh, H. J. Leu, R. B. Poeppel, E. Van Voorhees, G. T. Goudley, K. Winsley, and D. Shi, "Effect of Silver and Silver Oxide Additions on the Mechanical and Superconducting Properties of $YBa_2Cu_3O_{7-\delta}$ Superconductors," *J. Appl. Phys.*, **66** [7] 3154–59 (1989).

[2]K. C. Goretta, M. L. Kullberg, D. Bä, G. A. Risch, and J. L. Routbort, "Fracture Toughness of $YBa_2Cu_3O_x$ Containing Y_2BaCuO_5 and ZrO_2," *Supercond. Sci. Technol.*, **4**, 544–47 (1991).

[3]J. Joo, J. P. Singh, T. Warzynki, A. Grow, and R. B. Poeppel, "Role of Silver Addition on Mechanical and Superconducting Properties of High-T_c Superconductors," *Appl. Supercond.*, **2** [6] 401–10 (1994).

[4]K. C. Goretta *et al.*, "Processing and Properties of Bulk BiSrCaCuO Superconductors," *Appl. Supercond.*, **2** [6] 411–15 (1994).

[5]J. P. Singh, R. A. Guttschow, J. T. Dusek, and R. B. Poeppel, "Role of p_{O_2} in Microstructural Development and Properties of $YBa_2Cu_3O_x$ Superconductors," *J. Mater. Res.*, **7** [9] 2324–32 (1992).

[6]C.-Y. Chu, J. L. Routbort, N. Chen, A. C. Blondo, D. S. Kupperman, and K. C. Goretta, "Mechanical Properties and Texture of Dense Polycrystalline $Bi_2Sr_2CaCu_2O_x$," *Supercond. Sci. Technol.*, **5**, 306–12 (1992).

[7]K. C. Goretta, M. E. Loomans, L. J. Martin, J. Joo, R. B. Poeppel, and N. Chen, "Fracture of Dense, Textured $Bi_2Sr_2CaCu_2O_x$," *Supercond. Sci. Technol.*, **6**, 282–86 (1993).

[8]N. Murayama, Y. Kodama, S. Sakaguchi, and F. Wakai, "Mechanical Strength of Hot-Pressed Bi-Pb-Sr-Ca-Cu-O Superconductor," *J. Mater. Res.*, **7** [1] 34–47 (1992).

[9]L. A. Angurel, J. C. Diez, E. Martínez, J. I. Pea, G. F. de la Fuente, and R. Navarro, "Growth Rate Effects on Thin $Bi_2Sr_2CaCu_2O_{8+\delta}$ Textured Rods," *Physica C* (*Amsterdam*), **302**, 39–50 (1999).

[10]H. Yusheng, H. Yujing, L. Menglin, M. Sining, C. Liying, W. Ying, Z. Jincang, H. Alsheng, W. Jinsong, and Y. Xiaohua, "Fabrication, Characterization and Welding of Bi(Pb)-Sr-Ca-Cu-O Superconducting Fibres," *Supercond. Sci. Technol.*, **4**, 158–64 (1991).

[11]R. S. Fiegelson, D. Gazit, D. K. Fork, and T. H. Geballe, "Superconducting Bi-Ca-Sr-Cu-O Fibers Grown by the Laser-Heated Pedestal Growth Method," *Science*, **240**, 1642–45 (1988).

[12]G. de la Fuente, J. C. Diez, L. A. Angurel, J. I. Peña, A. Sotelo, and R. Navarro, "Wavelength Dependence in Laser Floating Zone Processing. A Case Study with Bi-Sr-Ca-Cu-O Superconductor," *Adv. Mater.*, **7** [10] 853–56 (1995).

[13]E. Martínez, "Imanación y Corrientes Críticas en Fibras Gruesas BSCCO: Texturado y Anclaje de Flujo"; Ph.D. Thesis. University of Zaragoza, 1997.

[14]"Standard Test Method for Splitting Tensile Strength of Cylindrical Concrete Specimens," ASTM Designation C 495–90. *1991 ASTM Annual Book of Standards*, American Society for Testing and Materials, Philadelphia, PA, pp. 266–69.

[15]C. Fanggao, M. Cankurtaran, G. A. Saunders, D. P. Almond, P. J. Ford, and A. Al-Kheffaji, "The Effects of Quenching and Lead Substitution on the Ultrasonic Wave Velocity and Attenuation in Bismuth Cuprate High T_c Superconductors," *Supercond. Sci. Technol.*, **3**, 546–55 (1990).

[16]M. Runde, J. L. Routbort, S. J. Rothman, K. C. Goretta, J. N. Mundy, X. Xu, and J. E. Baker, "Tracer Diffusion of Oxygen in $Bi_2Sr_2CaCu_2O_x$," *Phys. Rev. B: Condens. Matter*, **45**, 7375–82 (1992).

[17]P. Venugopal Reddy, "Elastic Behaviour of Some High T_c Superconductors"; pp. 69–123 in *Studies of High Temperature Superconductors*, Vol. 19. Nova Science Publishers, New York, 1996. □